Electronic Supplementary Material (ESI) for Physical Chemistry Chemical Physics.


# SUPPORTING INFORMATION

## Tuning the ambipolar charge transport properties of tricyanovinyl-substituted carbazole-based materials

Marta Reig,[a] Gintautas Bagdziunas,[b,c] Dmytro Volyniuk,[b] Juozas V. Grazulevicius,[b] and Dolores Velasco*[a]

[a] Grup de Materials Orgànics, Institut de Nanociència i Nanotecnologia (IN$^2$UB), Departament de Química Inorgànica i Orgànica, Secció de Química Orgànica, Universitat de Barcelona, Martí i Franquès 1, E-08028, Barcelona, Spain

[b] Department of Polymer Chemistry and Technology, Kaunas University of Technology, Radvilenu Plentas 19, LT-50254, Kaunas, Lithuania

[c] Department of Material Science and Electrical Engineering, State Research Institute Centre for Physical Sciences and Technology, Sauletekio Av. 3, LT-10257, Vilnius, Lithuania

** Corresponding author: D. Velasco. Phone: +34 93 403 92 60. Fax: +34 93 339 78 78. E-mail: dvelasco@ub.edu*

**Table of contents**

**Table S1.** Crystal data and structure refinement for 9-methyl-3-(1,2,2-tricyanovinyl)-9*H*-carbazole (**3**).

| | | |
|---|---|---|
| Identification code | 9-Methyl-3-(1,2,2-tricyanovinyl)-9*H*-carbazole | |
| Empirical formula | $C_{18}H_{10}N_4$ | |
| Formula weight | 282.30 | |
| Temperature | 100(2) K | |
| Wavelength | 0.71073 Å | |
| Crystal system | Monoclinic | |
| Space group | P 21/c | |
| Unit cell dimensions | a = 8.0644(5) Å | α= 90°. |
| | b = 25.5256(13) Å | β= 108.253(2)°. |
| | c = 7.0058(4) Å | γ = 90°. |
| Volume | 1369.57(14) $Å^3$ | |
| Z | 4 | |
| Density (calculated) | 1.369 $Mg/m^3$ | |
| Absorption coefficient | 0.085 $mm^{-1}$ | |
| F(000) | 584 | |
| Crystal size | 0.587 x 0.191 x 0.070 $mm^3$ | |
| Theta range for data collection | 2.660 to 26.400°. | |
| Index ranges | -10<=h<=10, -31<=k<=31, -7<=l<=8 | |
| Reflections collected | 12529 | |
| Independent reflections | 2783 [R(int) = 0.0516] | |
| Completeness to theta = 25.242° | 99.2 % | |
| Absorption correction | Semi-empirical from equivalents | |
| Max. and min. transmission | 0.7454 and 0.5571 | |
| Refinement method | Full-matrix least-squares on $F^2$ | |
| Data / restraints / parameters | 2783 / 0 / 200 | |
| Goodness-of-fit on $F^2$ | 1.081 | |
| Final R indices [I>2sigma(I)] | R1 = 0.0537, wR2 = 0.1287 | |
| R indices (all data) | R1 = 0.0737, wR2 = 0.1385 | |
| Extinction coefficient | n/a | |
| Largest diff. peak and hole | 0.358 and -0.301 $e.Å^{-3}$ | |

**Table S2.** Crystal data and structure refinement for 2-methoxy-9-methyl-3-(1,2,2-tricyanovinyl)-9*H*-carbazole (**4**).

| | | |
|---|---|---|
| Identification code | 2-Methoxy-9-methyl-3-(1,2,2-tricyanovinyl)-9*H*-carbazole | |
| Empirical formula | C19 H12 N4 O | |
| Formula weight | 312.33 | |
| Temperature | 100(2) K | |
| Wavelength | 0.71073 Å | |
| Crystal system | Monoclinic | |
| Space group | P 21/n | |
| Unit cell dimensions | a = 6.8946(9) Å | α= 90°. |
| | b = 16.799(2) Å | β= 93.493(6)°. |
| | c = 13.329(2) Å | γ = 90°. |
| Volume | 1540.9(4) $Å^3$ | |
| Z | 4 | |
| Density (calculated) | 1.346 $Mg/m^3$ | |
| Absorption coefficient | 0.087 $mm^{-1}$ | |
| F(000) | 648 | |
| Crystal size | 0.254 x 0.088 x 0.054 $mm^3$ | |
| Theta range for data collection | 2.425 to 26.388°. | |
| Index ranges | -8<=h<=8, -21<=k<=20, -16<=l<=16 | |
| Reflections collected | 18866 | |
| Independent reflections | 3156 [R(int) = 0.0615] | |
| Completeness to theta = 25.242° | 99.9 % | |
| Absorption correction | Semi-empirical from equivalents | |
| Max. and min. transmission | 0.7454 and 0.4743 | |
| Refinement method | Full-matrix least-squares on $F^2$ | |
| Data / restraints / parameters | 3156 / 0 / 219 | |
| Goodness-of-fit on $F^2$ | 1.033 | |
| Final R indices [I>2sigma(I)] | R1 = 0.0538, wR2 = 0.1098 | |
| R indices (all data) | R1 = 0.1112, wR2 = 0.1288 | |
| Extinction coefficient | n/a | |
| Largest diff. peak and hole | 0.346 and -0.311 $e.Å^{-3}$ | |

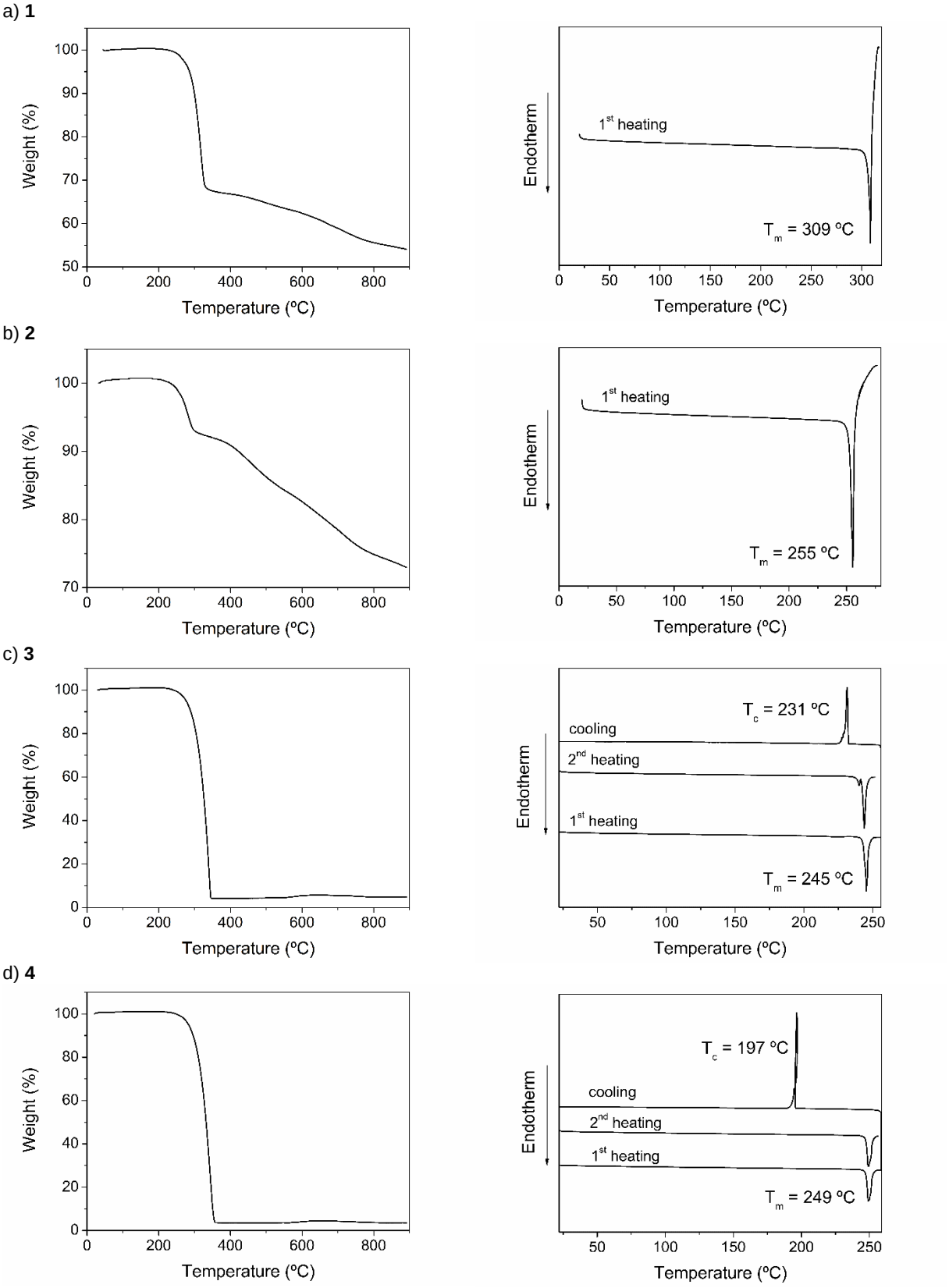


**Figure S1.** TGA (left) and DSC curves (right) for compounds **1**–**4** recorded at a scan rate of 20 °C $min^{-1}$ and 10 °C $min^{-1}$, respectively.

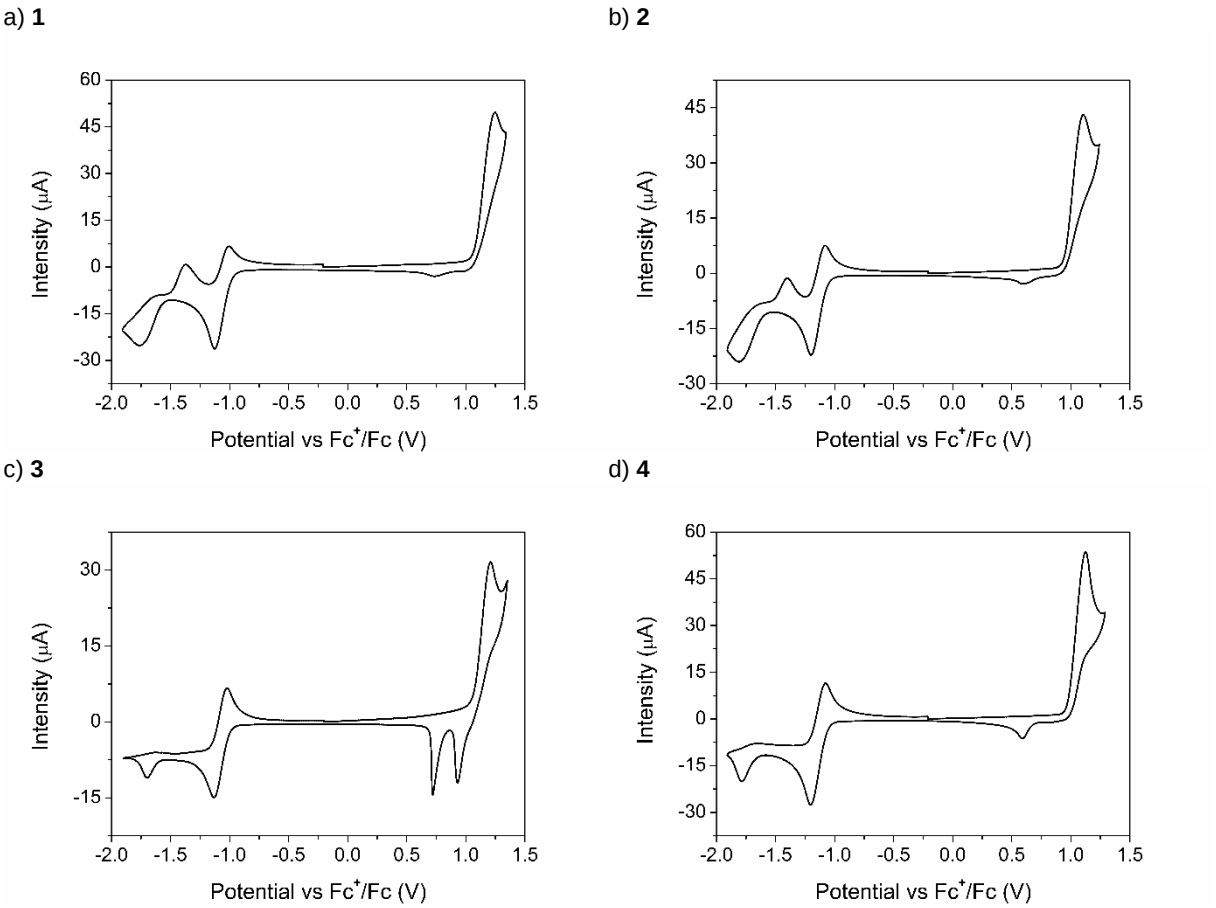


**Figure S2.** Cyclic voltammograms of compounds **1**–**4** recorded at 100 mV $s^{-1}$ in argon-purged dichloromethane solutions (1 mM) with $Ag/Ag^+$ (0.01 M $AgNO_3$) as the reference electrode.

a)

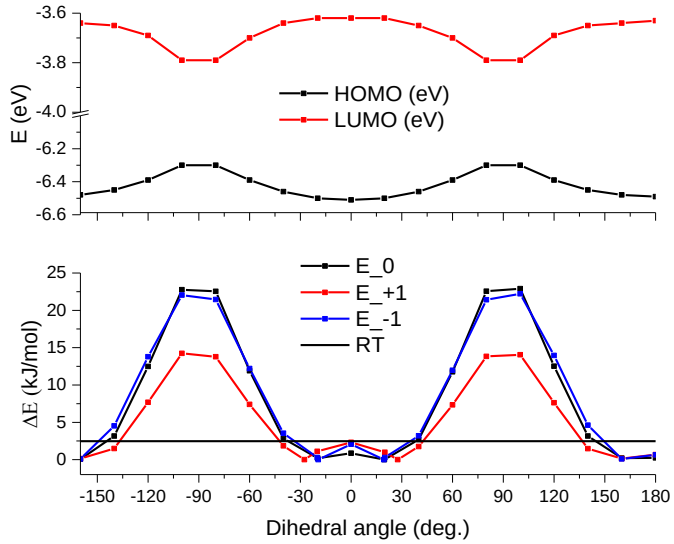


b)

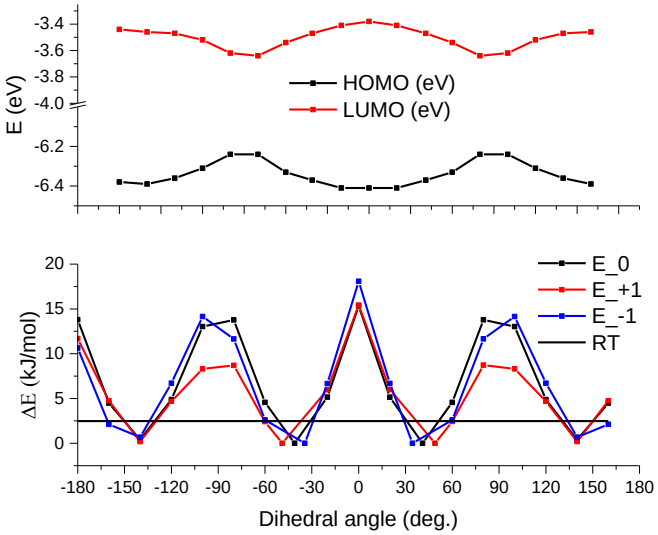


**Figure S3.** PES scans results of the neutral (E_0), cationic (E_+1) and anionic sates (E_-1) of molecules a) **3** and b) **4**. Line of $k_b$T energy is shown in black line.

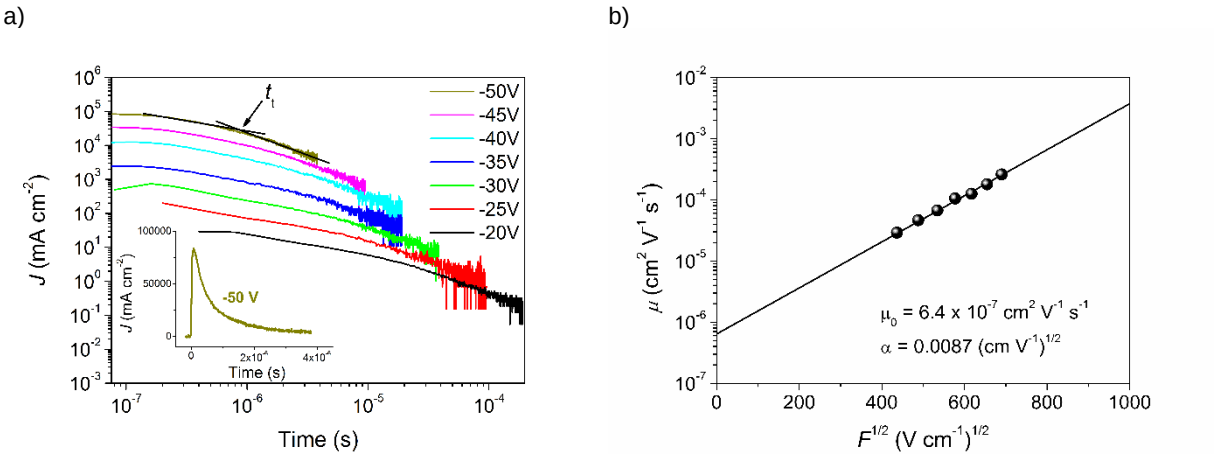


**Figure S4.** a) TOF transients for electron transport of the vacuum-deposited layer of compound **1** (d = 1.05 µm). Inset shows one transient curve in linear plot. b) Electric field dependencies of electron mobilities of the vacuum-deposited layer of compound **1**.

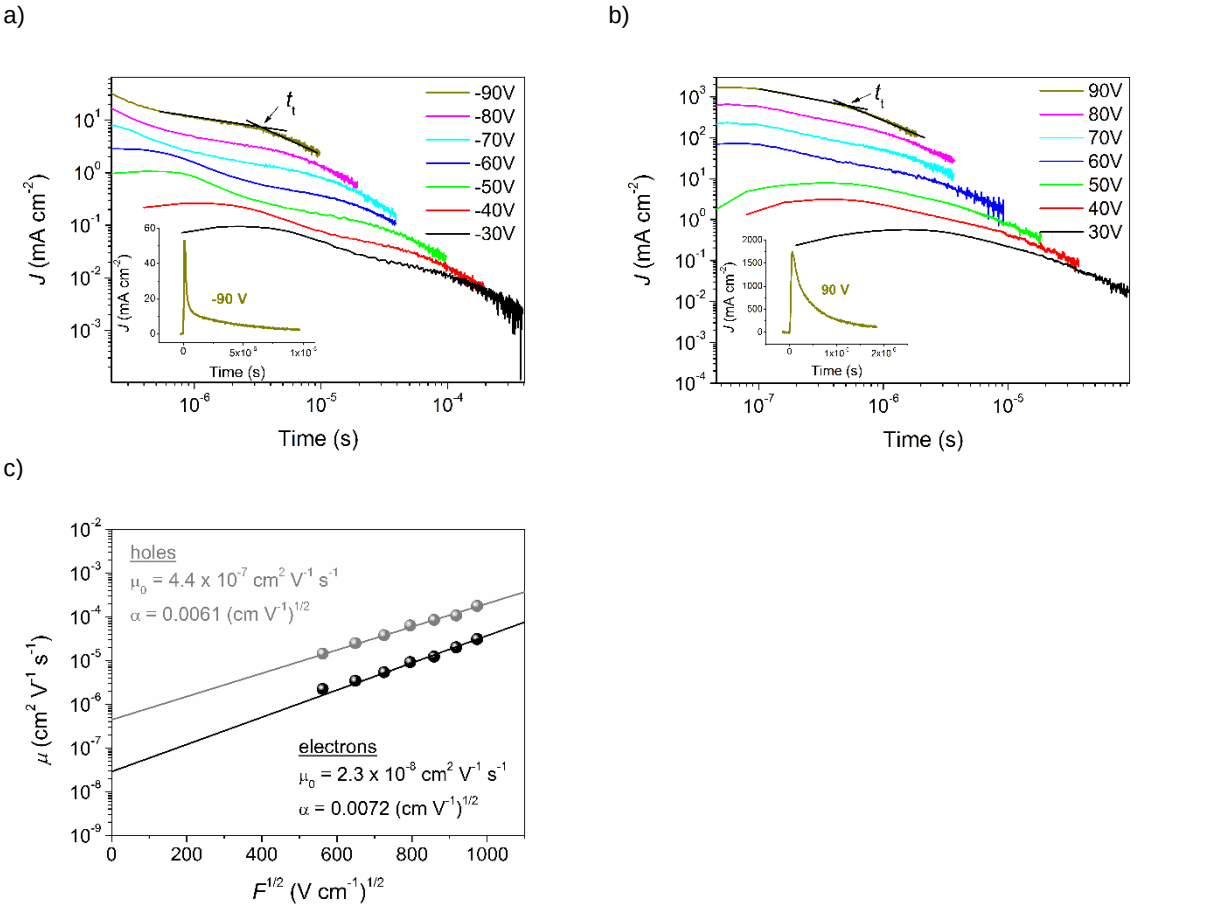


**Figure S5.** TOF transients for a) electron and b) hole transport of the vacuum-deposited layer of compound **2** (d = 0.95 µm). Inset shows one transient curve in linear plot. c) Electric field dependencies of electron and hole mobilities of the vacuum-deposited layer of compound **2**.

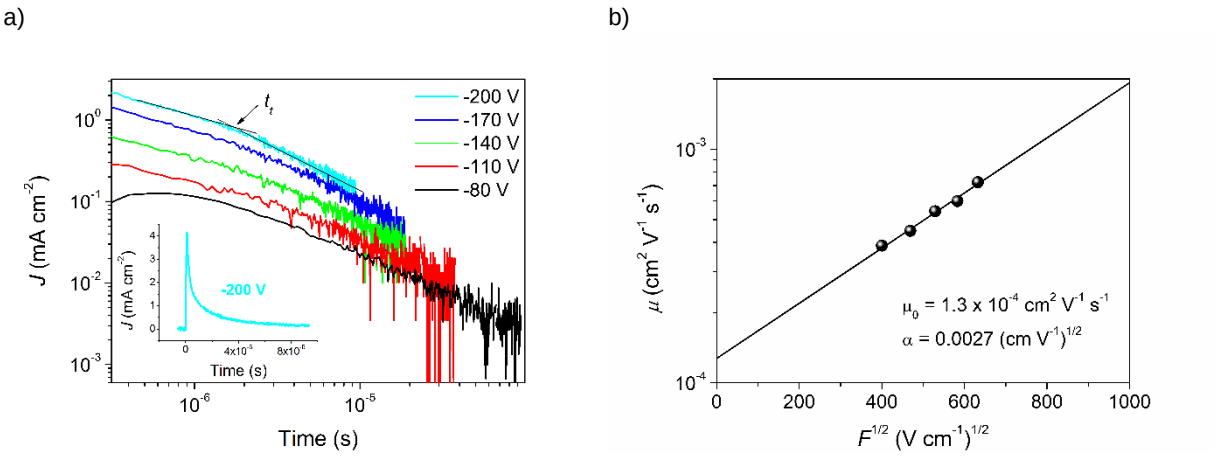


**Figure S6.** TOF transients for electron transport of the vacuum-deposited layer of compound **3** (d = 5.0 µm). Inset shows one transient curve in linear plot. c) Electric field dependencies of electron mobilities of the vacuum-deposited layer of compound **3**.

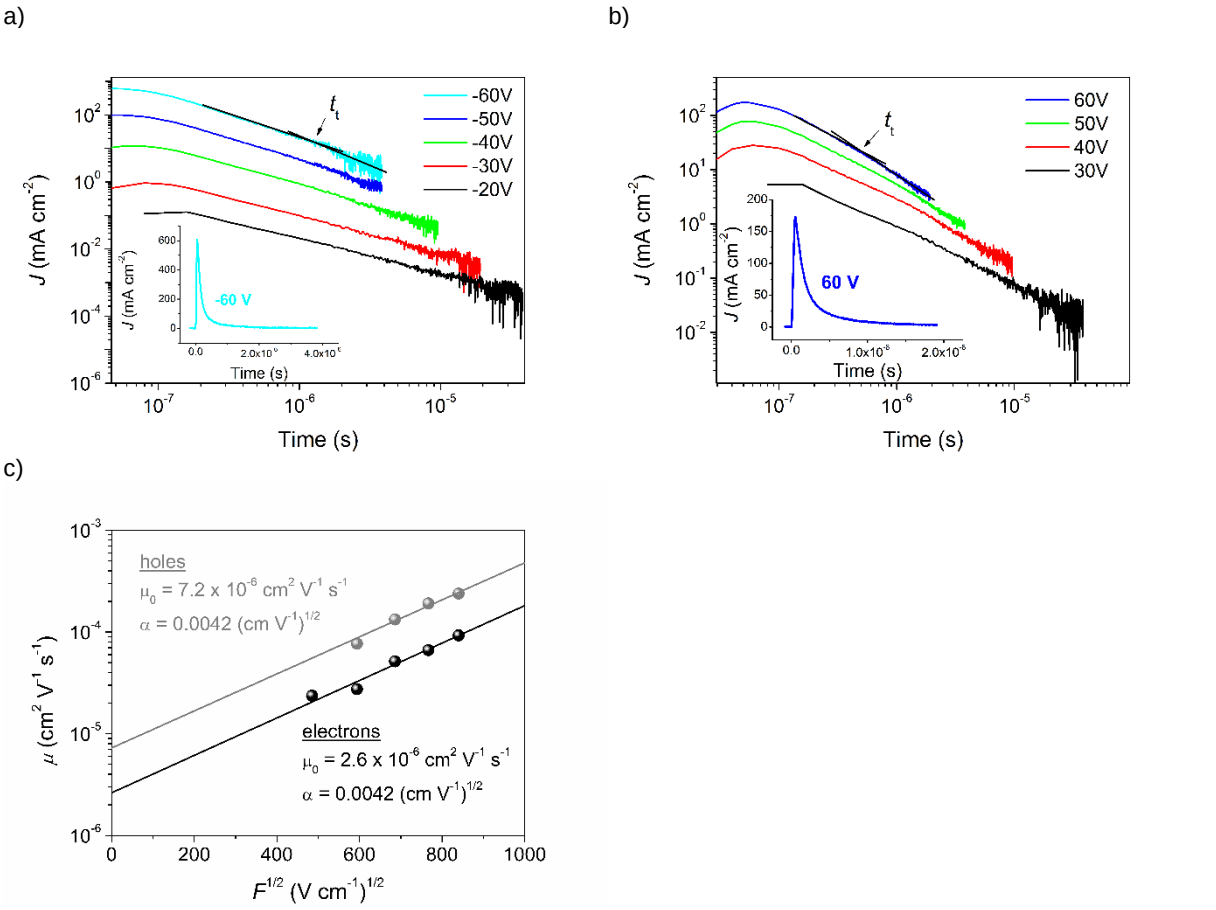


**Figure S7.** TOF transients for a) electron and b) hole transport of the vacuum-deposited layer of compound **4** (d = 0.85 µm). Inset shows one transient curve in linear plot. c) Electric field dependencies of electron and hole mobilities of the vacuum-deposited layer of compound **4**.

The electric field dependences for organic materials were previously described by the Gaussian disorder model, according to the following equation (S1): [1]

$$\mu = \mu_0 \exp[-(\frac{2\hat{\sigma}}{3})^2]\exp[C(\hat{\sigma}^2 - \Sigma^2)E^{1/2}] \quad \text{(S1)}$$

where $\sigma$ is the energy width of the hopping site manifold, Σ is the positional disorder, $C$ is an empirical constant, and $\hat{\sigma} = \sigma/k_B T$.

[1] H. Bässler, *Phys. Stat. Sol. B*, 1993, **175**, 15.

**Possible carrier hopping pathways between molecules for 3 and 4 and intermolecular interactions**

The most effective carrier hopping pathways for compounds **3** and **4**, which were selected for the charge mobility calculations, are shown in Figure 5 of the manuscript. However, other possible carrier hopping pathways between neighbouring molecules were also considered although they were finally removed from the modeling of mobility for the reasons mentioned below.

Adjacent molecules in pathway 2 of compound **3** from the crystal structure described here and the previously reported one[2] are connected via electrostatic C–H···NC hydrogen bonding (Figures S8 and S9). They show the highest coupling integrals for holes and electrons, but they are relatively unstable (i.e. the interaction energies are −17.7 and −15.4 kJ mol$^{-1}$, respectively) and present a lower probability in the amorphous state (Table S3). Neighbouring molecules in pathway 3 are connected via four C–H···NC intermolecular bonds, showing higher stability than in pathway 2, but displaying the lowest coupling integrals, which do not exceed the values of 20 meV.

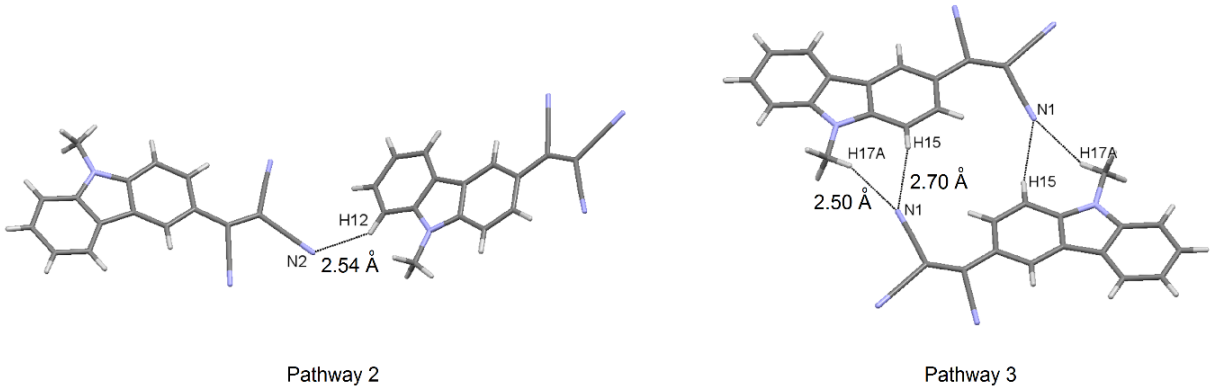


**Figure S8.** Possible carrier hopping pathways between neighbouring molecules and intermolecular interactions for the crystal structure of **3** reported here.

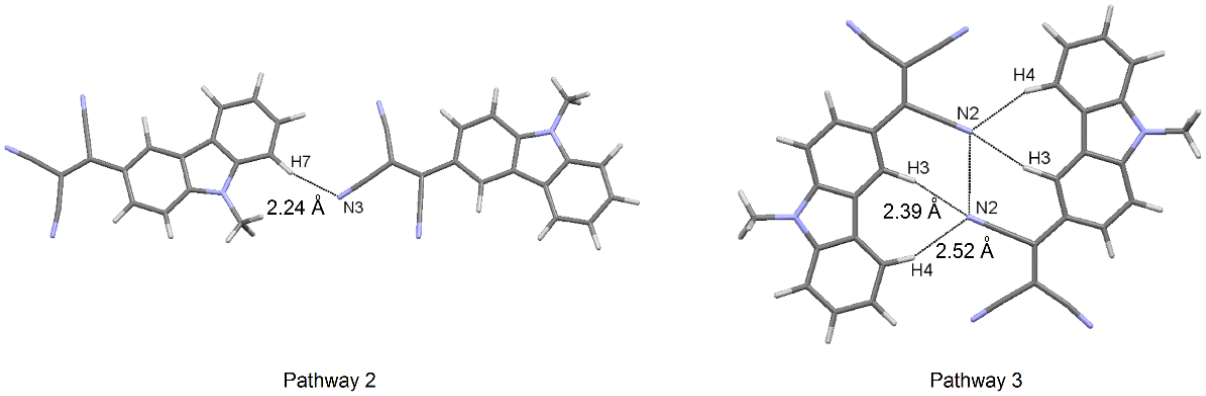


**Figure S9.** Possible carrier hopping pathways between neighbouring molecules and intermolecular interactions for the previously reported crystal structure[2] of **3**.

[2] E. G. Popova, L. A. Chetkina, B. V. Kotov, *Zhurnal Strukturnoi Khimii*, 1981, **22**, 116.

For compound **4**, neighbouring molecules in pathway 3 are connected via dipole-dipole interactions between CN groups, whereas dimers 4 and 5 via C–H···NC hydrogen bonding (Figure S10). Pathways 3–5 of compound **4** were excluded for the charge mobility calculations because neighbouring molecules show lower interaction energies (–33.0, –25.2 and –25.0 kJ $mol^{-1}$, respectively) than in pathways 1 and 2, together with very low probabilities, i.e. they do not exceeded the value of $10^{-13}$ (Table S3).

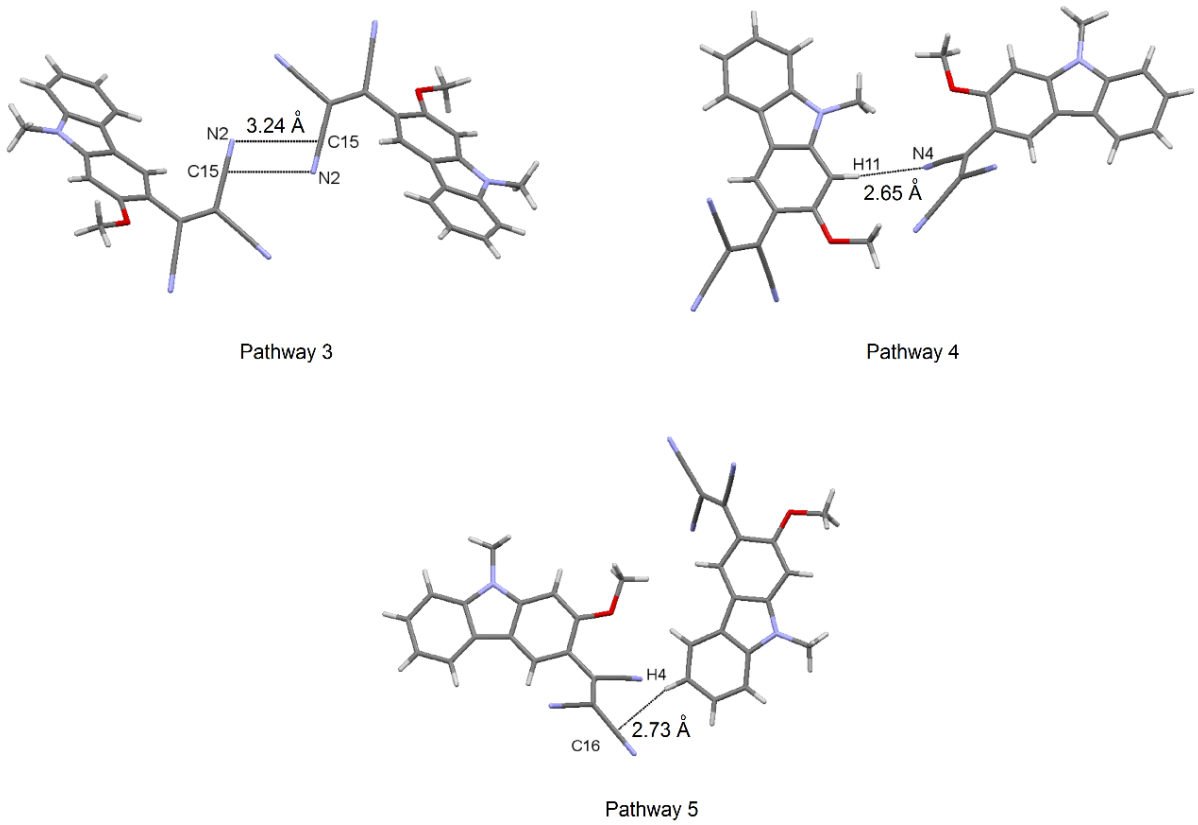


**Figure S10.** Possible carrier hopping pathways between neighbouring molecules and intermolecular interactions for the crystal structure of **4**.

**Table S3.** Theoretical calculation data of hole and electron mobilities of **3** and **4**.The data of the selected pathways for the calculation of charge carrier mobilities are shown in bold.

| Compd. | Pathway | d(D–D) [d] (Å) | d(A–A) [d] (Å) | $H_h$ [e] (meV) | $H_e$ [e] (meV) | $E_i$ [f] (kJ mol$^{-1}$) | $p_i$ [g] |
|---|---|---|---|---|---|---|---|
| **3**[a] | **1** | **7.56** | **3.42** | **47.4** | **140** | **–111** | **~1** |
| | 2 | 11.2 | 12.8 | 236 | 269 | –17.7 | $4.1\times10^{-17}$ |
| | 3 | 8.11 | 7.90 | 8.7 | 8.5 | –40.4 | $4.0\times10^{-13}$ |
| **3**[b] | **1** | **5.07** | **4.81** | **83.2** | **166** | **–76.9** | **~1** |
| | 2 | 13.6 | 13.5 | 242 | 299 | –15.4 | $1.7\times10^{-11}$ |
| | 3 | 11.0 | 7.56 | 6.9 | 12.9 | –44.7 | $2.3\times10^{-6}$ |
| **4**[c] | **1** | **4.60** | **8.32** | **63.1** | **21.8** | **–99.7** | **0.76** |
| | **2** | **3.87** | **9.84** | **121** | **8.4** | **–96.8** | **0.24** |
| | 3 | 13.6 | 9.58 | 26.3 | 88.5 | –33.0 | $1.6\times10^{-12}$ |
| | 4 | 9.51 | 8.94 | 65.0 | 405 | –25.2 | $6.8\times10^{-14}$ |
| | 5 | 10.3 | 8.56 | 16.8 | 38.3 | –25.0 | $6.1\times10^{-14}$ |

[a] Data estimated from the here reported crystal structure of **3** ($\lambda_+$ = 64.4 meV, $\lambda_-$ = 310 meV). [b] Data estimated from the previously reported crystal structure[2] of **3**. [c] Data estimated from the crystal structure of **4** ($\lambda_+$ = 249 meV, $\lambda_-$ = 369 meV). [d] Distance for pathway *i* between neighbouring donor-donor (D–D) for holes and acceptor-acceptor (A–A) moieties for electrons. [e] Coupling integrals for holes ($H_h$) and for electrons ($H_e$). [f] Interaction energy between neighbouring molecules. [g] Probability of charge migration.

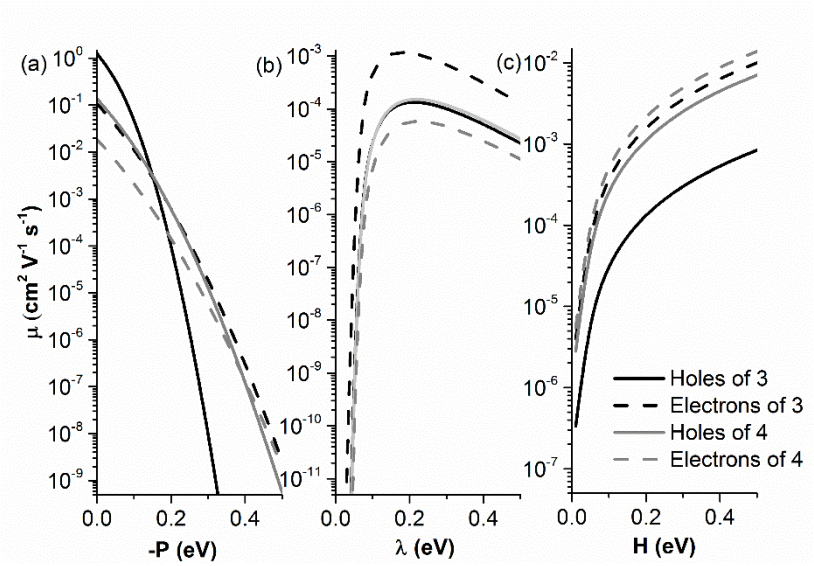


**Figure S11.** Visualization of the predicted hole and electron charge mobilities when changing only the polarization (a), reorganization energies (b) and the coupling integrals (c) for compounds **3** and **4** at $1.1\times10^7$ V m$^{-1}$ electric field.

**Table S4.** Computed dielectric constants, molecular volumes (with Van der Waals radius of 1Å) and static isotropic polarizabilities.

| Compound | α, Å$^3$ | V, Å$^3$ | ε |
|---|---|---|---|
| **3** | 39.3 | 368 | 3.4 |
| **4** | 40.3 | 403 | 3.2 |